The Astrophysical Journal, 696:1441–1447, 2009 May 10 doi:10.1088/0004-637X/696/2/1441

THE RELATION BETWEEN MORPHOLOGY AND DYNAMICS OF POOR GROUPS OF GALAXIES

Hrant M. Tovmassian[1] and M. Plionis[1,2]
[1] Instituto Nacional de Astrofísica Óptica y Electrónica, 72840 Puebla, Pue, Mexico; hrant@inaoep.mx
[2] Institute of Astronomy & Astrophysics, National Observatory of Athens, I. Metaxa & B. Pavlou, P. Penteli 152 36, Athens, Greece; mplionis@astro.noa.gr
Received 2008 December 19; accepted 2009 February 19; published 2009 April 24

ABSTRACT

We investigate the relation between the projected morphology and the velocity dispersion of groups of galaxies using two recently compiled group catalogs, one based on the Two Micron All Sky Survey redshift survey (Crook et al.) and the other on the Sloan Digital Sky Survey Data Release 5 galaxy catalog (Tago et al.). We analyze a suitable subsample of groups from each catalog selected such that it minimizes possible systematic effects. We find that the velocity dispersion of groups is strongly correlated with the group-projected shape and size, with elongated and larger groups having a lower velocity dispersion. Such a correlation could be attributed to the dynamical evolution of groups, with groups in the initial stages of formation, before virialization is complete, having small velocity dispersion, a large size, and an elongated shape that reflects the anisotropic accretion of galaxies along filamentary structures. However, we show that the same sort of correlations could also be reproduced in prolatelike groups, irrespective of their dynamical state, if the net galaxy motion is preferentially along the group elongation, since then the groups oriented close to the line of sight will appear more spherical, will have a small projected size and high-velocity dispersion, while groups oriented close to the sky plane will appear larger in projection, more elongated, and will have smaller velocity dispersion. Although both factors must play a role in shaping the observed correlations, we attempt to disentangle them by performing tests that relate only to the dynamical evolution of groups (i.e., calculating the fraction of early-type galaxies in groups and the projected group compactness). Indeed we find a strong positive (negative) correlation between the group velocity dispersion (group-projected major axis) with the fraction of early-type galaxy members. We conclude that (1) the observed dependences of the group velocity dispersion on the group-projected size and shape, should be attributed mostly to the dynamical state of groups, and (2) groups of galaxies in the local universe do not constitute a family of objects in dynamical equilibrium, but rather a family of cosmic structures that are presently at various stages of their virialization process.

Key words: galaxies: clusters: general – galaxies: evolution

Online-only material: color figures

1. INTRODUCTION

Poor groups of galaxies are the first-level structures of galaxies in the hierarchy of cosmic structure formation. Considerable effort has been put in identifying such objects in redshift surveys of galaxies and it has been found that a large number of galaxies in the local universe are indeed members of such groups (e.g., Huchra & Geller 1982; Tully 1987; Nolthenius & White 1987; Ramella et al. 2002; Merchán & Zandivarez 2002, 2005; Gal et al. 2003; Gerke et al. 2005; Lee et al. 2004; Lopes et al. 2004; Eke et al. 2004; Tago et al. 2006, 2008; Berlind et al. 2006; Crook et al. 2007; Yang et al. 2007).

The determination of the dynamical state and evolution of groups is an important step for investigating the hierarchical galaxy formation theories. Many dynamical and morphological studies have been restricted to compact groups (e.g., Kelm & Focardi 2004; Da Rocha et al. 2007; Coziol & Plauchu-Frayn 2007). The intrinsic elongated (mostly prolatelike) shape of groups (e.g., Hickson et al. 1984; Malykh & Orlov 1986; Orlov et al. 2001; Plionis et al. 2004, 2006; Wang et al. 2008) is a very important factor for the determination of their dynamical state (see, however, Robotham et al. 2007). Tovmassian et al. (1999) showed that the projected length and velocity dispersion of Hickson compact groups (Hickson 1982) are anticorrelated, and suggested that member galaxies in these groups possibly move preferentially along the group major axis in quasi-stable orbits (see also Tovmassian 2001, 2002). Using the Millennium simulation, Díaz-Gimenéz et al. (2008) have found a weak correlation between projected elongation and line-of-sight velocity dispersion in physically dense compact groups, but also in groups characterized as compact due to chance alignments along the line of sight.

Tovmassian & Chavushyan (2000) and Tovmassian et al. (2006) have found that members of loose groups in which compact groups are embedded, appear to move in similar elongated orbits around the common gravitational center of the corresponding group. However, such groups may represent only a special class and the study of generic poor groups is important for our understanding of their formation and evolution processes.

In this paper we study the relation between group morphology and dynamics, using as a measure of group morphology the projected axial ratio of the fitted ellipse and the projected group size, while as a measure of the group dynamical state we use its velocity dispersion and galaxy morphological content.

2. DATA AND METHODS

2.1. Group Sample Selection

In order to investigate group dynamics it is important to use groups not contaminated, as much as possible, by field galaxies. We want to stress that random projection of field galaxies over groups could affect their true shape and dynamical parameters, and also their morphological content. It is obvious that the probability of a group being significantly affected by random projections is inversely proportional to the group

galaxy membership, n_m. Projection of even one field galaxy may significantly alter the dynamical parameters of poor groups consisting of a few members. For example, Ramella et al. (2002) mention that 20%–60% of their groups which mainly consist of less than 10 galaxies, are expected to be contaminated by superpositions of field galaxies. Furthermore, the effect of discreteness in the determination of the shape of groups with a few members is severe (e.g., Paz et al. 2006; Plionis et al. 2006), a fact which results into artificially elongated shapes. Moreover, Robotham et al. (2007) claimed that poor groups with few galaxy members may have an oblate configuration. The expected galaxy orbits and therefore dynamics in oblate groups differ from that of groups with a prolatelike configuration, which has been shown to be the dominant group and cluster shape (e.g., Malykh & Orlov 1986; Plionis et al. 1991, 2004, 2006; de Theije et al. 1995; Basilakos et al. 2000; Cooray 2000; Sereno et al. 2006; Wang et al. 2008).

In this study, we use the Two Micron All Sky Survey (2MASS) high-density contrast (HDC) group catalog (Crook et al. 2007) which was constructed by a friends-of-friends algorithm (e.g., Huchra & Geller 1982) such that the groups correspond to an overdensity $\delta\rho/\rho \geqslant 80$. We have chosen to study this catalog and not the lower density contrast (LDC) one, which is based on $\delta\rho/\rho \geqslant 12$, since we believe that the HDC catalog is less prone to projection, interloper contamination, and contamination by the large-scale structures from which galaxies are accreted to the groups. We also use the group catalog constructed by Tago et al. (2008) from the Sloan Digital Sky Survey (SDSS) Data Release 5, which from now on we will tab as "Tago-SDSS." Although the authors do not provide the overdensity threshold to which their groups correspond, a crude calculation gives $\delta\rho/\rho \simeq 260$. The overdensity difference between the two group catalogs is reflected in their projected size distribution with the "Tago-SDSS" groups being significantly smaller than the 2MASS-HDC groups, as can be verified inspecting Figures 3–6 and 8 further below.

Taking into account the problems discussed in the beginning of this section, we wish to limit our study to groups with more than eight members ($n_m \geqslant 9$), and since our aim is to study poor groups we also put an upper limit of $n_m \leqslant 12$. Furthermore, by studying groups in a small n_m range we significantly reduce the variable, due to the different group membership, discreteness effects on their measured shape (e.g., Paz et al. 2006; Plionis et al. 2006).

One more important issue regarding mostly the high n_m groups is the fact that the increasing size of the friends-of-friends linking radii (radial and transverse), necessary to take into account the decrease of the selection function with redshift, tends to join at higher redshifts nearby (clustered) groups into single entities. Therefore, the probability that the groups are real dynamical entities should decrease with redshift. However, both of the group catalogs used (Crook et al. 2007; Tago et al. 2008) have been constructed taking special care for this effect and it appears that indeed the artificial trends, found in previous group catalogs (see the discussion in Plionis et al. 2004, 2006), have been significantly suppressed. Nonetheless, by visually inspecting the apparently large and high-velocity dispersion-rich groups, we have found that in quite a few occasions they appear to be the byproduct of joining neighboring groups. We would like to remind the reader that Rose (1977), Mamon (1986, 2008), and Walke & Mamon (1989) put forward the idea that some ordinary and compact groups could well be a result of such projection effect (see relevant recent works of

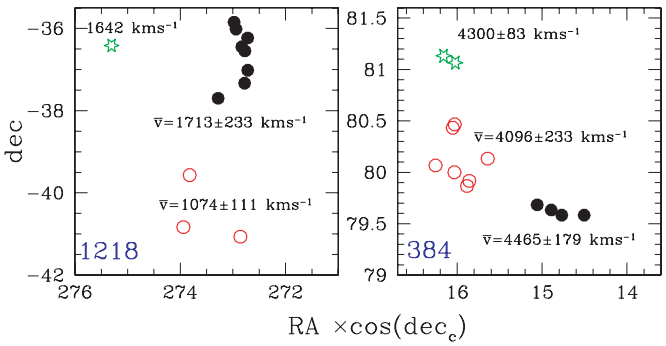

Figure 1. Equal area maps of two examples of 2MASS-HDC groups suspect of being composed of unrelated groups and field galaxies. Left panel: the group 1218, with $n_m = 12$, consists of two clearly distant subgroups at a projected separation of $\sim$1.4 h^{-1} Mpc (at the mean redshift of the whole group) and a mean velocity difference of $\sim$700 km s^{-1}. This group is the only clearly "problematic" group in our $n_m = 9$–12 sample. Right panel: the group 384, with $n_m = 13$, possibly consists of three separate groups with mean radial velocities as indicated in the plot. The projected distance (at the mean redshift of the whole group) of the northern and southern subgroups from the central one is $\sim$2 and $\sim$1.3 h^{-1} Mpc, respectively.

(A color version of this figure is available in the online journal.)

Díaz-Gimenéz et al. 2008 and Brasseur et al. 2009). Of the groups with $9 \leqslant n_m \leqslant 12$ we have found, in the 2MASS-HDC sample, only one that clearly falls in this category (No. 1218; see Figure 1) which we exclude from our analysis. Indeed, the projected distribution of members of this group shows that eight of its members compose a relatively compact group with mean $V = 1713 \pm 233$ km s^{-1}, and a wide triplet located at a projected distance of $\sim$1.4 h^{-1} Mpc to the south with mean $V = 1074 \pm 111$ km s^{-1} (distances are measured at the mean redshift of the whole group).[3] As another example, we present in Figure 1 the map of 2MASS-HDC group No. 384 with a multiplicity $n_m = 13$ which could consist of two to three probably unrelated groups.

We will also analyze groups (with $n_m \geqslant 9$) based on their estimated virial masses since the magnitude-limited nature of the 2MASS galaxy redshift survey implies that groups of the same multiplicity but at different redshifts correspond to different intrinsic richness. Indeed, the difference of the $K_{\rm total}$ apparent magnitude (Jarrett et al. 2000) between the brightest and faintest galaxy in the 2MASS-HDC groups with, for example, nine members is $\approx$3.5 mag for nearby groups with $cz \approx 300$ km s^{-1}, and systematically decreases to about 1.5 mag for distant groups with $cz \approx 7000$ km s^{-1}. This shows that faint group members are missed as a function of increasing redshift and thus the distant groups, of apparently the same multiplicity as nearby ones, are intrinsically richer in members above a given luminosity threshold. However, if we assume that the missed faint galaxies randomly sample the distribution of group member velocities, then the mass estimate of the groups will not be systematically affected by the omission of these fainter galaxies and therefore performing an analysis of low- and intermediate-mass groups (i.e., excluding the apparently massive systems which could be artificial) circumvents the previously mentioned problems. Note, however, that the above assumption may not be valid for virialized groups in which dynamical friction has played a relatively important role, and in which case their mass may be underestimated.

In order to have as much as possible a representative sample of the true underlying local group population and to minimize

[3] Throughout this work, we use $H_0 = 100\,h$ km s^{-1} Mpc^{-1} with $h = 0.73$.

the above-mentioned redshift-dependent systematic biases, we have chosen to study from the Tago-SDSS catalog the groups within $z \leqslant 0.043$. Note that the 2MASS-HDC group sample is by construction defined in the local universe ($z \leqslant 0.033$).

2.2. Shape and Dynamics Measures

We determine the projected group shape diagonalizing the moments of inertia tensor, which we construct by weighting each member galaxy by $1/K_{\rm total}$, with $K_{\rm total}$ the apparent K-band galaxy magnitude. This is done in order to weight more the luminous (and thus massive) galaxies, which dominate in shaping the group gravitational potential.

First, the galaxy equatorial positions are transformed into an equal-area coordinate system, centered on the group center of mass (which we determine using obviously the $1/K_{\rm total}$ weighting scheme). We then evaluate the moments

$$I_{11} = \sum_i w_i \left(r_i^2 - x_i^2\right)$$
$$I_{22} = \sum_i w_i \left(r_i^2 - y_i^2\right) \quad (1)$$
$$I_{12} = I_{21} = -\sum_i w_i x_i y_i$$

with w_i ($=1/K_{\rm total}$) the statistical weight of each member galaxy and r_i the distance of the ith galaxy from the group center of mass. Note that because the inertia tensor is symmetric, we have $I_{12} = I_{21}$. Diagonalizing the inertia tensor

$$\det(I_{ij} - \lambda^2 M_2) = 0 \quad (M_2 \text{ is a } 2 \times 2 \text{ unit matrix}), \quad (2)$$

we obtain the eigenvalues λ_1, λ_2, from which we define the principal axial ratio of the configuration under study by $q = \lambda_2/\lambda_1 (\equiv b/a)$, with $\lambda_1 > \lambda_2$.

As a measure of the size of the group, we also calculate the mean projected galaxy–galaxy separation and a variant (see below) which we use to estimate the group virial mass (only for the Tago et al. groups, since for the 2MASS-HDC groups the relevant values are provided by the catalog).

The group virial radius, used to determine the group mass, is

$$R_v = \frac{n_m(n_m - 1)}{\sum_{i=1}^{n_m - 1} \sum_{j=i+1}^{n_m} [D_L \tan(\delta\theta_{ij})]^{-1}}, \quad (3)$$

where D_L is the luminosity distance of the group (using $\Omega_\Lambda = 0.7$, $\Omega_{\rm m} = 0.3$, $h = 0.73$), and $\delta\theta_{ij}$ is the angular (i, j)-pair separation. Using the group velocity dispersion and R_v, we can estimate the group's virial mass according to

$$M_v = \frac{3\pi}{2} \frac{\sigma_v^2 R_v}{G}. \quad (4)$$

Note that R_v is significantly smaller than the maximum or the mean group galaxy–pair separation. In what follows, we will use as the major axis of each group, a, its mean galaxy–pair separation and as its minor axis: $b = aq$.

3. GROUP MORPHOLOGY–DYNAMICS RELATION

3.1. Background Framework

Do we expect to find a priori any morphology–dynamics relation in a sample of self-gravitating groups of galaxies which are in dynamical equilibrium? The answer is probably no, since in such a case the velocity dispersion of the group should reflect its virial mass, while the group shape should be quasi-spherical since relaxation processes will have (mostly) isotropized the initial anisotropic group phase space. If, however, a group morphology–dynamics relation is found, then it could be due to either of the two possible causes (or a combination of both).

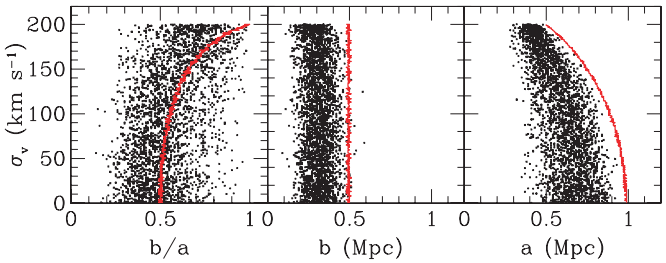

Figure 2. Expected morphology–dynamics correlations due to the random orientation with respect to the line of sight of prolate spheroids with intrinsic $q = 0.5$ and major axis $a = 1$ Mpc. The red line is the expected theoretical curves, while the black points represent random realizations in which each group is sampled by 10 "galaxies."

(A color version of this figure is available in the online journal.)

1. The groups of galaxies in the sample are not all virialized but at different evolutionary stages, and therefore it is possible to find a correlation between their velocity dispersion (as a measure of their dynamical state) and the group size and axial ratio, since a group at its early stages of formation will have a larger size, with respect to their final dynamical relaxed state, and it will be more elongated reflecting the initial anisotropic accretion of matter along filamentary structures (e.g., West 1994).
2. Since groups of galaxies are prolatelike, as has been found by numerous studies (see the introduction), and if galaxies move predominantly along the group elongation, then the size, the axial ratio, and the velocity dispersion of the groups will depend on the group orientation with respect to the line of sight. The nearer is the orientation of the three-dimensional major axis of a group to the line of sight, the smaller will appear its size, the larger its axial ratio, and velocity dispersion (Tovmassian et al. 1999, 2006, and references therein). In effect, performing a simple Monte Carlo simulation in which we randomly orient with respect to the line of sight, 1000 intrinsically prolate groups with $q = 0.5$, $a = 1$ Mpc, and velocity dispersion $\sigma_v = 200$ km s^{-1} strictly along its major axis, we obtain in Figure 2 the red curves, which constitute the theoretical expectation in the presence of no discreetness. If now we sample each group by 10 "galaxies," we again obtain very significant q–σ_v and a–σ_v correlations but with a large scatter. It is important to note that (1) in this model the a–σ_v correlation is stronger than the q–σ_v correlation while no b–σ_v correlation expected, and (2) the observed scatter in Figure 2 is solely due to sampling randomly each Monte Carlo group by 10 "galaxies." More scatter should be expected, however, in a more realistic situation in which the intrinsic range of group sizes and velocity dispersions would have been taken into account.

In fact, the intrinsic spread in group sizes could effectively mask the possible morphology–dynamics correlations, and thus even a weak correlation should be considered as a hint of a true underlying effect.

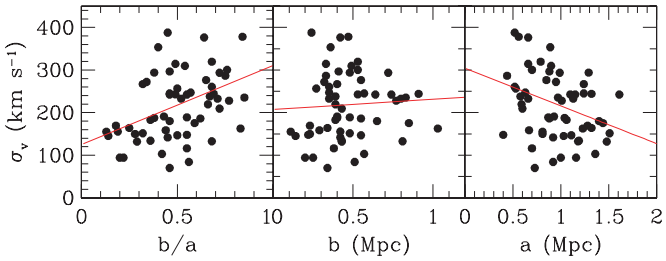

Figure 3. Morphology–dynamics correlations of the 2MASS-HDC groups: from left to right the q–σ_v, b–σ_v, and a–σ_v scatter diagrams.

(A color version of this figure is available in the online journal.)

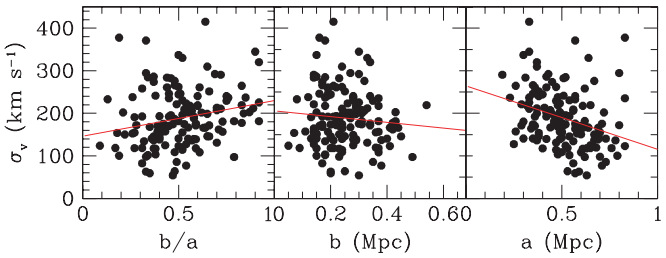

Figure 4. Morphology–dynamics correlations of the Tago-SDSS groups: from left to right the q–σ_v, b–σ_v, and a–σ_v scatter diagrams.

(A color version of this figure is available in the online journal.)

3.2. Possible Systematic Effects

Any systematic redshift dependence of σ_v and group size, introduced by the convolution of the friends-of-friends group-finding algorithm and the magnitude-limited nature of the underlying galaxy catalogs (see the discussion in Plionis et al. 2006), produces a dependence of the group size and the velocity dispersion with redshift (at higher z's you get large groups with higher σ_v), which could also results in an artificial correlation between a and σ_v, but such that $a \propto \sigma_v$ (opposite to what predicted by either of the possibilities discussed previously).

We have tested whether such bias is present in the presently analyzed group samples (as has been found in previous group samples; see the discussion in Plionis et al. 2004, 2006) and found that for the 2MASS-HDC samples there is a relatively weak σ_v–z correlation ($R = 0.29$ with $\mathcal{P} = 0.02$) and an insignificant a–z correlation ($R = 0.18$ with $\mathcal{P} = 0.18$), probably due to the special effort put by the authors to reduce such systematics (Crook et al. 2007). The positive σ_v–z correlation could well be due to the expected volume effect (i.e., at higher z's, a large fraction of the group mass function is sampled). Regarding the SDSS-Tago groups, we find no correlation whatsoever between either σ_v nor a with redshift, again an indication that the authors managed to suppress the systematics from which many other group catalogs suffer.

3.3. Results

In Figures 3 and 4, we plot the scatter diagrams between the group shape parameters and their velocity dispersion for both group catalogs analyzed. It is evident that we do find the qualitatively expected correlations which are quite strong and significant in both catalogs of groups. The Pearson correlation coefficients R and corresponding random probabilities $\mathcal{P}$ for the considered group subsamples are presented in Table 1. It is evident that the velocity dispersion σ_v of groups increases with increasing q, while it decreases with increasing the group major axis a (while the opposite is expected if it would have been due to the systematics discussed previously). An additional systematic effect that acts in the direction of diluting a positive q–σ_v correlation is that, within any n_m bin, the range of group virial masses traced will tend to induce an anticorrelation between q and σ_v, since more massive halos are more elongated (lower q) and have a higher velocity dispersion with respect to less-massive halos (e.g., Jing & Suto 2002; Kasun & Evrard 2005; Allgood et al. 2006; Bett et al. 2007; Ragone-Figueroa & Plionis 2007; Wang et al. 2008). This implies that the observed shape–dynamics correlation is, in effect, stronger than that observed. Note also that a weak but nonsignificant correlation is found between the groups minor axis and velocity dispersion. As we will see further below (Figure 4), this is due to the lower mass groups which do not show a negative b–σ_v correlation.

Probably a more instructive view of the morphology–dynamics correlations, which is free of the bias of mixing poor nearby and richer distant groups of the same multiplicity (n_m), is to divide the group samples into ranges of mass, according to Equation (4). To this end, we use all groups with $n_m \geqslant 9$ and divided each group sample in four bins of mass, excluding groups with $M > 10^{14}\ h^{-1}\ M_\odot$, which actually correspond to clusters. A further reason to exclude the high-mass groups is the contamination problem we have identified in some apparently high-velocity dispersion groups (see Figure 1).

In Figures 5 and 6 and in Table 2, we present the same morphology–dynamics correlations as before, but dividing the groups in bins of mass. The correlations are now more evident, with different mass range groups occupying a clearly delineated region in the q–σ_v, b–σ_v, and a–σ_v planes. Although the number of 2MASS-HDC groups in each mass range is small, the q–σ_v correlations are systematic and significant (with the exception of the highest mass range which could be affected by the previously

Table 1
The Pearson Correlation Coefficients R and Corresponding Random Probabilities $\mathcal{P}$ for the 2MASS-HDC and Tago-SDSS Group Samples with $9 \leqslant n_m \leqslant 12$

Catalog	No.	q–σ_v		b–σ_v		a–σ_v	
		R	$\mathcal{P}$	R	$\mathcal{P}$	R	$\mathcal{P}$
2MASS-HDC	59	0.396	0.0019	0.112	0.398	−0.361	0.0046
Tago-SDSS	140	0.260	0.0019	−0.05	0.557	−0.380	3×10^{-6}

Table 2
The Pearson Correlation Coefficients R and Corresponding Random Probabilities $\mathcal{P}$ for the 2MASS-HDC and Tago-SDSS Group Samples in Different Mass Ranges

2MASS-HDC							
$\log M/M_\odot$ Range	No.	q–σ_v		b–σ_v		a–σ_v	
		R	$\mathcal{P}$	R	$\mathcal{P}$	R	$\mathcal{P}$
12–13	7	0.71	0.07	0.78	0.036	0.61	0.14
13–13.5	18	0.49	0.04	0.31	0.21	−0.34	0.16
13.5–13.75	23	0.48	0.02	−0.54	0.008	−0.85	$<10^{-6}$
13.75–14	29	0.06	0.74	−0.55	0.002	−0.84	$<10^{-6}$
Tago-SDSS							
$\log M/M_\odot$ Range	No.	q–σ_v		b–σ_v		a–σ_v	
		R	$\mathcal{P}$	R	$\mathcal{P}$	R	$\mathcal{P}$
12–13	78	0.24	0.032	−0.19	0.09	−0.54	$<10^{-6}$
13–13.25	70	0.33	0.006	−0.35	0.003	−0.79	$<10^{-6}$
13.25–13.5	71	0.00	0.96	−0.45	10^{-5}	−0.66	$<10^{-6}$
13.5–13.8	36	0.64	10^{-5}	0.04	0.79	−0.69	2×10^{-6}

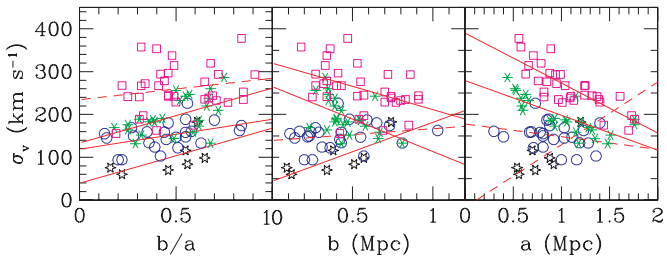

Figure 5. Morphology–dynamics correlations of the 2MASS-HDC groups in different mass ranges: from left to right the q–σ_v, b–σ_v, and a–σ_v scatter diagrams. The stars correspond to $12 < \log M/M_\odot \leqslant 13$, blue open circles to $13 < \log M/M_\odot \leqslant 13.5$, green filled circles to $13.5 < \log M/M_\odot \leqslant 13.75$, and magenta open squares to $13.75 < \log M/M_\odot \leqslant 14$.

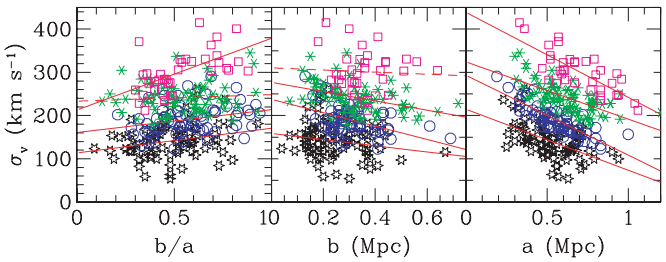

Figure 6. Morphology–dynamics correlations of the Tago-SDSS groups in different mass ranges: from left to right the q–σ_v, b–σ_v, and a–σ_v scatter diagrams. The stars correspond to $12 < \log M/M_\odot \leqslant 13$, blue open circles to $13 < \log M/M_\odot \leqslant 13.25$, green multiple crosses to $13.25 < \log M/M_\odot \leqslant 13.5$, and magenta open squares to $13.5 < \log M/M_\odot \leqslant 13.75$.

mentioned problems). The a–σ_v and b–σ_v correlations are present only for groups with $M \geqslant 10^{13.5}\ h^{-1}\ M_\odot$. Similar and more significant correlations are found in the case of the Tago-SDSS groups. Here, however, the a–σ_v correlations are extremely significant, while there is also a significant correlation of the minor axis with velocity dispersion.

3.4. Orientation or Virialization?

For the orientation paradigm to work in producing the observed correlations, it is also important to have galaxies moving predominantly along the prolatelike group major axis. Such galaxy motions are generally expected in the hierarchical structure formation scenario, where groups and clusters of galaxies are formed by anisotropic accretion and merging along filamentary large-scale structures (e.g., West 1994). However, the possible predominance of such galaxy orbits would also imply that the groups are not virialized, since virialization would mix the phase space and erase (mostly) the memory of the initial directional accretion (see, however, van Haarlem & van de Weygaert 1993).

It is interesting to point out that the observed a–σ_v correlations are generally more significant than those of q–σ_v, a fact which agrees also with the expectations of the orientation paradigm (see Figure 2), and could be attributed to the dispersion of the minor axis, b, which does not depend on the group orientation.

Therefore, although both discussed causes of the observed group morphology–dynamics correlations should be at work, we attempt to disentangle which of the two, if any, dominates. To this end we consider two tests, one based on the morphological content of groups of galaxies, since a proxy of their dynamical state should be their morphological content, and the other based on the expectation of the virialization process to compactify the initial dispersed group morphology.

3.4.1. Morphological Content of Groups

It has been shown that galaxies in clusters evolve mainly by dynamical interactions and merging (e.g., Goto 2005). It also appears that mergers, strangulation as well as interactions with the hot diffuse gas (for the richest groups) act in the group environment and affect the morphology and gas content of member galaxies (e.g., Barnes 1985; Zabludoff & Mulchaey 1998; Hashimoto & Oemler 2000; Coziol & Plauchu-Frayn 2007; Rasmussen et al. 2008). The efficiency of galaxy interactions in altering the morphology and gas content of galaxy group members depends on their relative velocity, being more efficient in low-velocity dispersion groups (e.g., Mamon 1992), which implies that such processes should be relatively frequent in the early stages of the group dynamical evolution. While galaxy interactions and merging occur, contemporary the host group evolves dynamically and therefore the fraction of E/S0 galaxies should appear high in dynamically advanced (high-velocity dispersion) groups. Indeed, the fraction of E/S0 galaxies, $f_{\rm E/S0}$, in groups appears to increase with increasing group velocity dispersion (e.g., Tovmassian et al. 2004; Aguerri et al. 2007), a fact which could also be viewed as a manifestation of the known *density–morphology* relation at the groups scale (Postman & Geller 1984).

Therefore, if we also verify for our current group samples a correlation between morphological content, $f_{\rm E/S0}$, and group velocity dispersion then this would clearly suggest that the observed range of velocity dispersions is related mostly to the group dynamical state and not to the group orientation (in which case no $f_{\rm E/S0}$–σ_v correlation is expected). We apply this test to the well defined 2MASS-HDC groups with $n_m = 9$–12. We used those groups with 9–10 members for which the morphological type of no more than one member galaxy was unknown, and groups with 11–12 members, the morphological types of no more than two galaxies were unknown. We took morphological types of member galaxies from the NASA/IPAC Extragalactic Database (NED). The total number of groups used is 33 and their σ_v–$f_{\rm E/S0}$ scatter diagram is presented in the left panel of Figure 7 (we also show in this plot with an empty dot the excluded No. 1218 group, suspected of being contaminated by multipole groups; see Section 2.1) and it is evident that $f_{\rm E/S0}$ strongly increases with increasing σ_v. The Pearson correlation coefficient and random probability are $R = 0.54$ and $\mathcal{P} = 3 \times 10^{-4}$, respectively, showing that the σ_v–$f_{\rm E/S0}$ correlation is indeed very significant.

During virialization, the groups should become more compact and their major axis should decrease. If this is so, then the σ_v–$f_{\rm E/S0}$ correlation implies that there should also be a a–σ_v correlation. Indeed, the right panel of Figure 7 shows the corresponding correlation with coefficient $R = 0.44$ and random probability $\mathcal{P} = 0.01$. The q–$f_{\rm E/S0}$ correlation is weak and not significant which could well be due to the influence of the large dispersion of the group minor axis, b.

3.4.2. Minor Axis and Group-projected Size

In the orientation paradigm, the increase of the velocity dispersion takes place with corresponding decrease of the projected major axis of a group, while the minor axis remains unchanged (see Figure 2). Meanwhile, during virialization both the projected major and minor axes, and thus the projected surface (S) of a self-gravitating system should decrease becoming more compact. Indeed, we have found that the projected minor axes of most of the analyzed samples of groups decrease with increasing

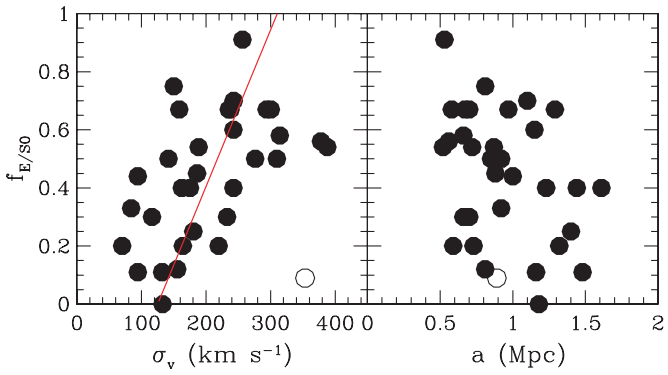

Figure 7. Dependence of the fraction $f_{E/S0}$ of early-type galaxies in groups on the group velocity dispersion σ_v (left panel) and major-axis size (right panel).
(A color version of this figure is available in the online journal.)

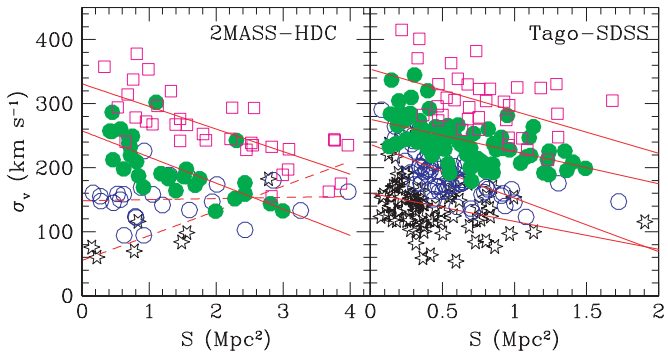

Figure 8. Dependence of the projected group surface (S) on the group velocity dispersion, σ_v for subsamples of different masses. Left panel: 2MASS-HDC groups (symbols as in Figure 5). Right panel: SDSS-Tago groups (symbols as in Figure 6).
(A color version of this figure is available in the online journal.)

velocity dispersion. Note, however, that projection effects and the presence of interlopers will affect more the projected minor axis, with respect to the major axis, of an intrinsically elongated group, and thus weaken any true correlations between b and σ_v. This, as well as low-number statistics, could be the reasons why the low-mass 2MASS-HDC groups (see Figure 5) do not show a negative b–σ_v correlation.

Obviously, the a–σ_v and b–σ_v correlations translate into a S–σ_v correlation with a rate of variation, in the virialization case, which is higher than that caused by orientation (in which case only a decreases with increasing σ_v). In Figure 8, we present the S–σ_v correlations for the mass-defined 2MASS-HDC and Tago-SDSS groups. It is evident that, depending on group virial mass, the group surface varies by 5–8 times within the range covered by the group velocity dispersion. The corresponding variation in the case of the orientation paradigm is expected to be $\sim 1/q$, which means that for the observed groups (which have $\langle q \rangle \sim 0.5$) the expected surface variation, within the indicated velocity dispersion range, is ~ 2 (as seen also in the right panel of Figure 2), significantly smaller than what observed.

4. CONCLUSIONS

If a family of cosmic structures are all virialized, there is no reason to find any significant morphology–dynamics correlations. Such a correlation may be expected in two cases: (1) if the galaxy group members have a net motion predominantly along the group elongation, as expected in dynamical young groups which form by anisotropic accretion of matter along filamentary large-scale structures, then due to projection there must be a positive correlation between the group axial ratio q and the group radial velocity dispersion, and a negative correlation between the projected group major axis and the group radial velocity dispersion, and (2) if virialization is currently at work, which will tend to compactify and sphericalize the initial volume from which the structures form, as well as increase its velocity dispersion.

We searched for such correlations using 2MASS-HDC (Crook et al. 2007) and SDSS Data Release 5 (Tago et al. 2008) catalogs of groups. In order to avoid discreteness and interloper contamination effects we have performed two analyses, one based solely on group samples defined by their apparent multiplicity ($n_m = 9$–12) and the other based on samples defined in bins of group virial mass.

We found significant negative a–σ_v and positive q–σ_v correlations, although the observed correlations could have been substantially weakened by many effects, among which also a distance-dependent bias by which at larger redshifts the detected group length and velocity dispersion increases artificially. However, we have verified that the analyzed groups, due to the specific care taken by the authors that constructed them, do not suffer significantly of this effect.

We have also found a positive and significant correlation between the early-type galaxy content and the group velocity dispersion, as well as a negative correlation between the early-type galaxy content and the group major axis. These correlations indicate that the cause of the group morphology–velocity dispersion trend should be attributed mostly to the dynamical evolution of structures and not to their orientation with respect to the line of sight.

Our final conclusion, based on all available evidence regarding the observed group morphology–dynamics and morphological content–dynamics relations, is that the groups of galaxies in the local universe do not constitute a family of objects in dynamical equilibrium, but rather a family of cosmic structures that are presently at various stages of their virialization process. We also expect that the observed group morphology–dynamics correlations are affected by the group orientation with respect to the line of sight, but such an effect works in the same direction as the virialization process.

M.P. acknowledges funding by CONACyT grant 2005-49878. This research has made use of the NASA/IPAC Extragalactic Database (NED) which is operated by the Jet Propulsion Laboratory, California Institute of Technology, under contract with the National Aeronautics and Space Administration. We thank Cinthia Ragone-Figueroa, Gary Mamon, and Manuel Merchán for useful suggestions and comments.

REFERENCES

Aguerri, J. A. L., Sanchez-Janssen, R., & Muñoz-Tunon, C. 2007, A&A, 471, 17
Allgood, B. F., Flores, A., Primack, J. R., Kravtsov, A. V., Wechsler, R. H., Faltenbacher, A., & Bullock, J. S. 2006, MNRAS, 367, 1781
Barnes, J. 1985, MNRAS, 215, 517
Basilakos, S., Plionis, M., & Maddox, S. J. 2000, MNRAS, 316, 779
Berlind, A. A., et al. 2006, ApJS, 167, 1
Bett, P., Eke, V., Frenk, C. S., Jenkins, A., Helly, J., & Navarro, J. 2007, MNRAS, 376, 215
Brasseur, C. M., McConnachie, A. W., Ellison, S. L., & Patton, D. R. 2009, MNRAS, 392, 1141
Cooray, R. A. 2000, MNRAS, 313, 783
Coziol, R., & Plauchu-Frayn, I. 2007, AJ, 133, 2630

Crook, A. C., Huchra, J. P., Martimbeau, N., Masters, K., Jarrett, T., & Macri, L. M. 2007, ApJ, 655, 790
Da Rocha, C., Ziegler, B. L., & Mendes de Oliveira, C. 2007, in IAU Symp. 235, Galaxy Evolution Across the Hubble Time, ed. F. Combes & J. Palous (Cambridge: Cambridge Univ. Press), 199
de Theije, P. A. M., Katgert, P., & van Kampen, E. 1995, MNRAS, 273, 30
Díaz-Gimenéz, E., Ragone-Figueroa, C., Muriel, H., & Mamon, G. A. 2008, arXiv:0809.3483
Eke, V. R., et al. 2004, MNRAS, 348, 866
Gal, R. R., de Carvalho, R. R., Lopes, P. A. A., Djorgovski, S. G., Brunner, R. J., Mahabal, A., & Odewahn, S. C. 2003, AJ, 125, 2064
Gerke, F. B., et al. 2005, ApJ, 625, 6
Goto, T. 2005, MNRAS, 359, 1415
Hashimoto, Y., & Oemler, A., Jr. 2000, ApJ, 530, 652
Hickson, P. 1982, ApJ, 255, 382
Hickson, P., Ninkov, Z., Huchra, J. P., & Mamon, G. A. 1984, in Clusters and Groups of Galaxies, ed. F. Mardirossian, G. Giuricin, & M. Mezzetti (Dordrecht: D. Reidel Pub.), 367
Huchra, J. P., & Geller, M. J. 1982, ApJ, 257, 423
Jarrett, T. H., Chester, T., Cutri, R., Schneider, S., Skrutskie, M., & Huchra, J. P. 2000, AJ, 119, 2498
Jing, Y. P., & Suto, Y. 2002, ApJ, 574, 538
Kasun, S. F., & Evrard, A. E. 2005, ApJ, 629, 781
Kelm, B., & Focardi, P. 2004, A&A, 418, 937
Lee, B. C., et al. 2004, AJ, 127, 1811
Lopes, P. A. A., de Carvalho, R. R., Gal, R. R., Djorgovski, S. G., Odewahn, S. C., Mahabal, A. A., & Brunner, R. J. 2004, AJ, 128, 1017
Malykh, S. A., & Orlov, V. V. 1986, Astofizika, 24, 445
Mamon, G. A. 1986, ApJ, 307, 426
Mamon, G. A. 1992, ApJ, 401, L3
Mamon, G. A. 2008, A&A, 486, 113
Merchán, M. E., & Zandivarez, A. 2002, MNRAS, 335, 216
Merchán, M. E., & Zandivarez, A. 2005, ApJ, 630, 759
Nolthenius, R., & White, S. D. M. 1987, MNRAS, 225, 505
Orlov, V. V., Petrova, A. V., & Tarantaev, V. G. 2001, MNRAS, 325, 133
Paz, D. J., Lambas, D. G., Padilla, N., & Merchan, M. 2006, MNRAS, 366, 1503
Plionis, M., Barrow, J. D., & Frenk, C. S. 1991, MNRAS, 249, 662
Plionis, M., Basilakos, S., & Ragone-Figueroa, C. 2006, ApJ, 650, 770
Plionis, M., Basilakos, S., & Tovmassian, H. M. 2004, MNRAS, 352, 1323
Postman, M., & Geller, M. J. 1984, ApJ, 281, 95
Ragone-Figueroa, C., & Plionis, M. 2007, MNRAS, 377, 1785
Ramella, M., Geller, M. J., Pisani, A., & da Costa, L. N. 2002, AJ, 123, 2976
Rasmussen, J., Ponman, T. J., Verdes-Montenegro, L., Yun, M. S., & Sanchayeeta, B. 2008, MNRAS, 388, 1245
Robotham, A., Phillips, S., & de Propris, R. 2007, ApJ, 672, 834
Rose, J. A. 1977, ApJ, 211, 311
Sereno, M., De Filippis, E., Longo, G., & Bautz, M. W. 2006, ApJ, 645, 170
Tago, E., Einasto, J, Saar, E., Tempel, E., Einasto, M., Vennik, J., & Muller, V. 2008, A&A, 479, 927
Tago, E., et al. 2006, Astron. Nachr., 327, 365
Tovmassian, H. M. 2001, PASP, 113, 543
Tovmassian, H. M. 2002, Astron. Nachr., 323, 488
Tovmassian, H. M., & Charushyan, V. H. 2000, AJ, 119, 1687
Tovmassian, H. M., Martinez, O., & Tiersch, H. 1999, A&A, 348, 693
Tovmassian, H. M., Plionis, M., & Andernach, H. 2004, ApJ, 617, L111
Tovmassian, H. M., Plionis, M., & Torres-Papaqui, J. P. 2006, A&A, 456, 839
Tully, R. B. 1987, ApJ, 321, 280
van Haarlem, M., & van de Weygaert, R. 1993, ApJ, 418, 544
Walke, D. G., & Mamon, G. A. 1989, A&A, 225, 291
Wang, Y., Yang, X., Mo, H. J., Li, C., van den Bosch, F. C., Fan, Z., & Chen, X. 2008, MNRAS, 385, 1511
West, M. J. 1994, MNRAS, 268, 79
Yang, X., Mo, H. J., van den Bosch, F. C., Pasquali, A., Li, C., & Barden, M. 2007, ApJ, 671, 153
Zabludoff, A. I., & Mulchaey, J. S. 1998, ApJ, 496, 39